

## REMOTE SENSING OF H FROM *ULYSSES* AND *GALILEO*

W. PRYOR, I. STEWART, K. SIMMONS, M. WITTE, J. AJELLO, K. TOSKIBA,  
D. MCCOMAS and D. HALL

*LASP, University of Colorado, Boulder, CO 80303, U.S.A.*

**Abstract.** We model interplanetary H Lyman- $\alpha$  ( $L\alpha$ ) observations from *Galileo* UVS (Ultraviolet Spectrometer) and EUVS (Extreme Ultraviolet Spectrometer) (Hord *et al.*, 1992) and the *Ulysses* interstellar neutral gas (GAS) instrument (Witte *et al.*, 1992). EUVS measurements near solar maximum (max) in 1990–1992 have a peaked brightness maximum upwind due to a rather isotropic solar wind charge-exchange ionization pattern ( $A = 0$ –0.25). GAS measurements from solar minimum (min) in 1997 have a plateau in the upwind direction that we model using *Ulysses* SWOOPS (solar wind plasma experiment) solar min data on solar wind density and velocity at different heliographic latitudes. The isotropic ionization pattern deduced from EUVS at solar max may be consistent with recent SWOOPS results (McComas *et al.*, 2000b, c) that high speed solar wind is absent at high latitudes during solar max. *Galileo* and *Ulysses*  $L\alpha$  data favor higher H temperatures (15 000–18 000 K) than previous models.

### 1. Introduction

$L\alpha$  signal comes from solar  $L\alpha$  photons scattered from interstellar wind (ISW) H flowing from upwind: ecliptic longitude  $254^\circ$  and latitude  $6^\circ$  (Witte *et al.*, 1996). H gas properties assumed ‘at infinity’ in our hot models (e.g., Thomas, 1978) are density  $n \sim 0.17 \text{ cm}^{-3}$ , velocity  $v = 20 \text{ km s}^{-1}$ , and temperature  $T = 8000$ – $18\,000 \text{ K}$ . We previously used  $8000 \text{ K}$  (Bertaux *et al.*, 1985); but the SOHO SWAN H cell finds  $T \sim 11\,000$ – $13\,000 \text{ K}$  (Costa *et al.*, 1999). We test this new SWAN result for  $T$ .

ISW H near the sun is lost mostly by charge exchange with solar wind protons, and by some solar EUV photoionization, leaving a cavity depleted in slow H that scatters solar  $L\alpha$ . The interplanetary  $L\alpha$  brightness along a line of sight is:

$$4\pi I = \int_0^\infty n(s)p(\varphi(s))g(s)q[\Theta(s)]ds \quad (1)$$

and depends on solar  $L\alpha$  flux through scattering coefficient  $g$ , on the slow H density  $n$ , phase function  $p$  as a function of scattering angle  $\varphi$ , and multiple scattering correction  $q$  as a function of the angle  $\Theta$  from upwind to sun to field point (Ajello *et al.*, 1994). We model solar  $L\alpha$  flux and radiation pressure effects using UARS SOLSTICE data and He 1083 nm images (Pryor *et al.*, 1996, 1998a, b) to study  $\tau$ ,



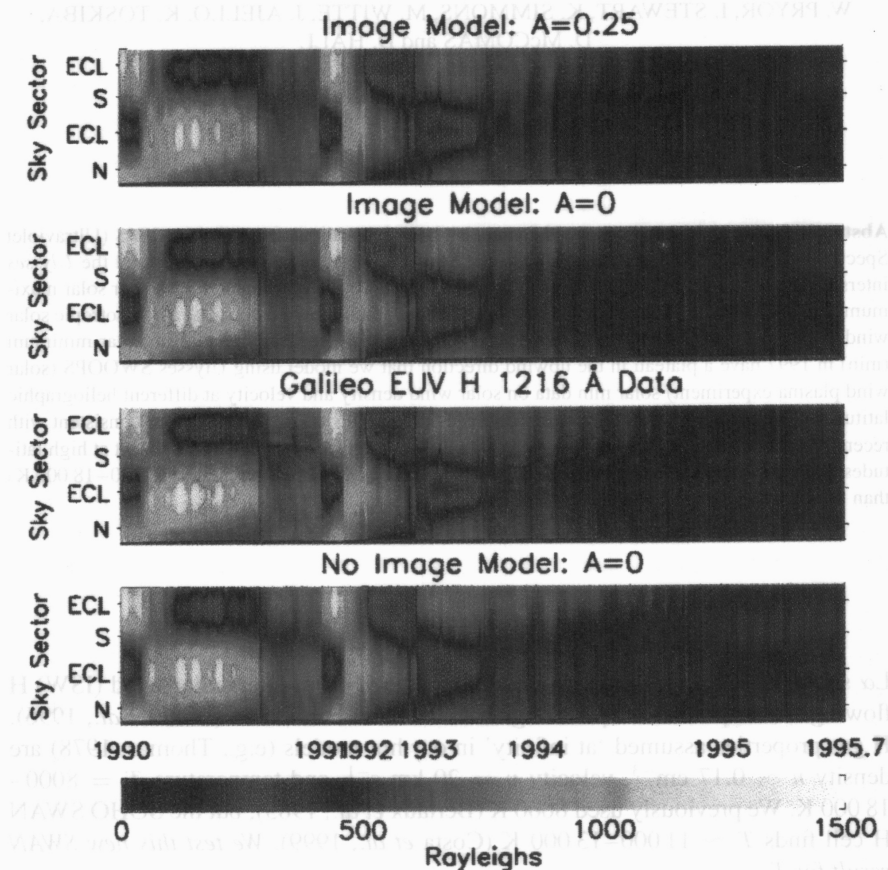


Figure 1. Galileo EUVS  $L\alpha$  data from 1990–1995 are shown with 3 models (all at 15 000 K): the top two panels show the ‘image model’ for  $A = 0.25$  and  $A = 0$ , that uses He 1083 nm images to model solar  $L\alpha$  at each latitude and longitude; the overly symmetric ‘no image’ model (similar to the symmetric solar model of Pryor *et al.*, 1996) uses  $A = 0$  with the time-varying anisotropic  $L\alpha$  values measured in the ecliptic plane and a lower polar flux equal to 85% of the 27-day running average ecliptic values. The upwind ecliptic plane is usually brightest. Galileo was downwind after launch in 1989, and again in December 1990 and December 1992. Galileo was almost upwind in mid-1990, mid-1991, and from late-1993 to 1995. Average model brightness was scaled to average data brightness for each date. Two comets occur in the 1990 data; the second one (extra yellow dot near ECL) is Comet Levy. Discontinuities in brightness in the time dimension are from data-taking gaps.

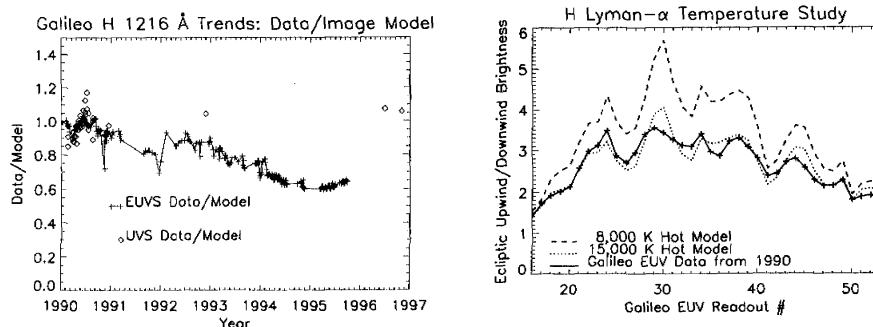


Figure 2. Left: the trend (data/15 000 K model) is shown for the *Galileo* EUVS and UVS data sets. EUVS declined in  $L\alpha$  sensitivity. Right: the 1990 EUVS upwind to downwind brightness ratio from days 124 to 291 is better matched by 15 000 K 'at infinity' in the hot model than 8000 K. In both plots  $A = 0$ .

the H lifetime against solar wind charge exchange; and  $n$  and  $T$ , the density and temperature of the gas at large distances upwind (inside the heliopause).

*Galileo* UVS  $L\alpha$  maps from 1990 (Ajello *et al.*, 1994) and 1992 show downwind conditions at the last solar max. *Galileo* EUVS  $L\alpha$  data (Pryor *et al.*, 1992, 1996) from 1990–1995 cover great circles through the ecliptic poles, at nearly right angles to the sun-spacecraft line. EUVS at times measures both upwind and downwind (Figure 3). These data show the latitude dependence of  $L\alpha$  brightness, which depends on the global mass flux distribution of the solar wind. The *Ulysses* GAS experiment also maps interplanetary  $L\alpha$  (Pryor *et al.*, 1998b). A December 1997 GAS map that was obtained near the ecliptic plane at solar min is also sensitive to the solar wind latitude distribution. Hot model results are compared to EUVS data in Figures 1 and 2, to UVS data in Figures 2 and 3, and to GAS data in Figures 4 and 5.

## 2. *Galileo* EUVS and UVS Conclusions for the Previous Solar Max

- A model with a latitude-invariant H lifetime (almost symmetric solar wind mass flux:  $A = 0.00$  or  $0.25$ ) and  $T = 15\,000$  K fits EUVS spatial and temporal variations well, 1990–1995 (Figure 1). 15 000 K is favored over 8000 K for small solar wind asymmetry parameter  $A$  (Figure 2). The  $A = 0$  image model is better thru 1992,  $A = 0.25$  after that.
- UVS trends are well-fit, but not EUVS, implying EUVS lost sensitivity (Figure 2).
- The solar max (December 1990) UVS antisun map (Figure 3) favors  $A = 0$ – $0.25$  (latitude-invariant solar wind mass flux).
- The declining phase (December 1992) UVS antisun map (Figure 3) favors  $A = 0.25$  over  $A = 0.0$  (enhanced ecliptic solar wind mass flux).

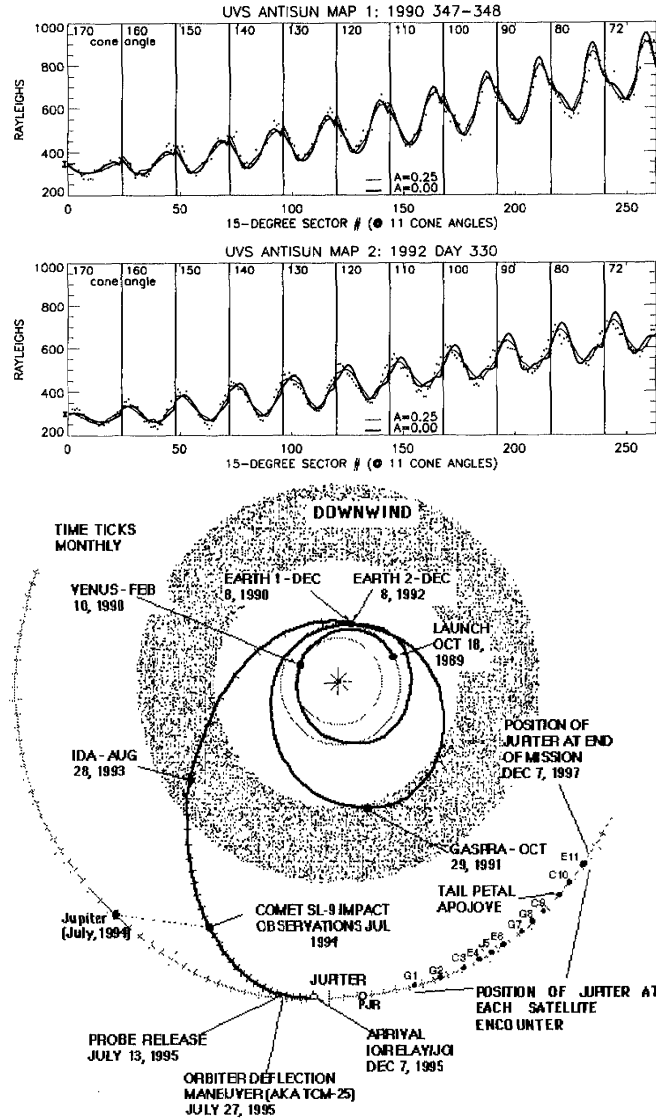


Figure 3. Top: UVS  $L\alpha$  maps (Ajello *et al.*, 1994) of the downwind hemisphere are modeled with image models with  $T = 15\,000$  K and  $A = 0$  or  $A = 0.25$ . The data from each cone angle begins and ends near ecliptic north, and passes near ecliptic south at the mid-point.  $1 - \sigma$  error bars are shown for the 1st data point in each map (to the left for clarity). The 1990 solar max map was obtained from spacecraft heliocentric ecliptic coordinates  $(x, y, z) = (0.13, 0.95, -0.01)$  AU and fits equally well with  $A = 0$  or  $A = 0.25$ . The dimmer 1992 declining phase map from coordinates  $(0.50, 0.92, 0.02)$  AU) favors  $A = 0.25$ . Figure 4 explains  $A = 0$  and  $A = 0.25$ . Bottom: *Galileo* orbit 1989–1997.

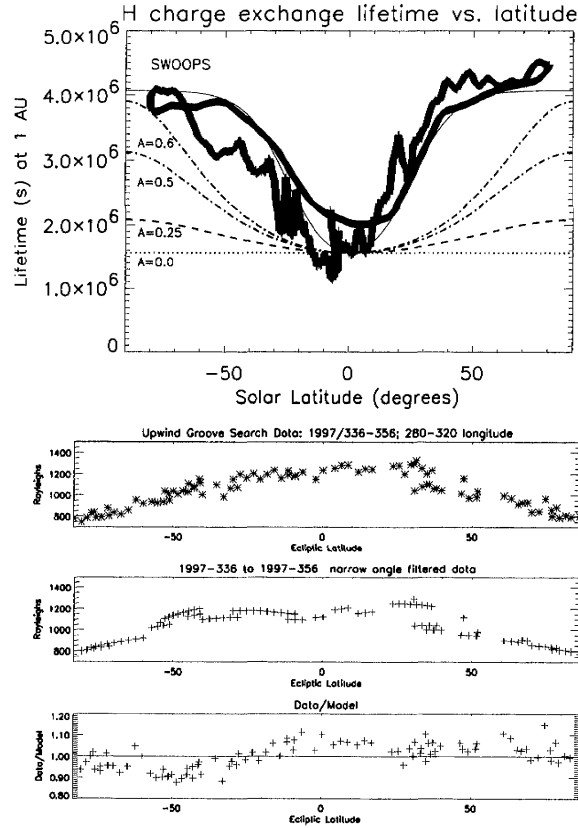


Figure 4. Top: H lifetime variation with heliographic latitude is shown for  $A = 0, 0.25, 0.5$ , and  $0.6$  and for a symmetric fit to *Ulysses* SWOOPS data (McComas *et al.*, 1999). Bottom: upwind GAS data in the direction range  $280\text{--}320$  longitude have been selected to search for an ecliptic groove. Data remaining after filtering obvious stars from the 1997 GAS  $L\alpha$  map are compared to a  $15\,000\text{ K}$  model using the fit to SWOOPS data shown at top. SWOOPS data show enhanced charge-exchange in the south, as do GAS  $L\alpha$  data.

—Low  $A$  values at solar max may fit in with recent SWOOPS data that high speed solar wind is absent at high latitudes at solar max (McComas *et al.*, 2000b, c).

### 3. *Ulysses* GAS and Charge Exchange Losses

A ‘groove’ in SWAN  $L\alpha$  data in  $L\alpha$  near the upwind ecliptic plane is due to enhanced  $H - H^+$  charge exchange at low latitudes at solar min (Bertaux *et al.*, 1997). GAS upwind data from December 2–22, 1997 (solar min) in Figure 4 show a plateau at low latitudes, with a weak groove. This differs from EUVS solar max data that were sharply peaked in the upwind ecliptic (Pryor *et al.*, 1992, 1996).

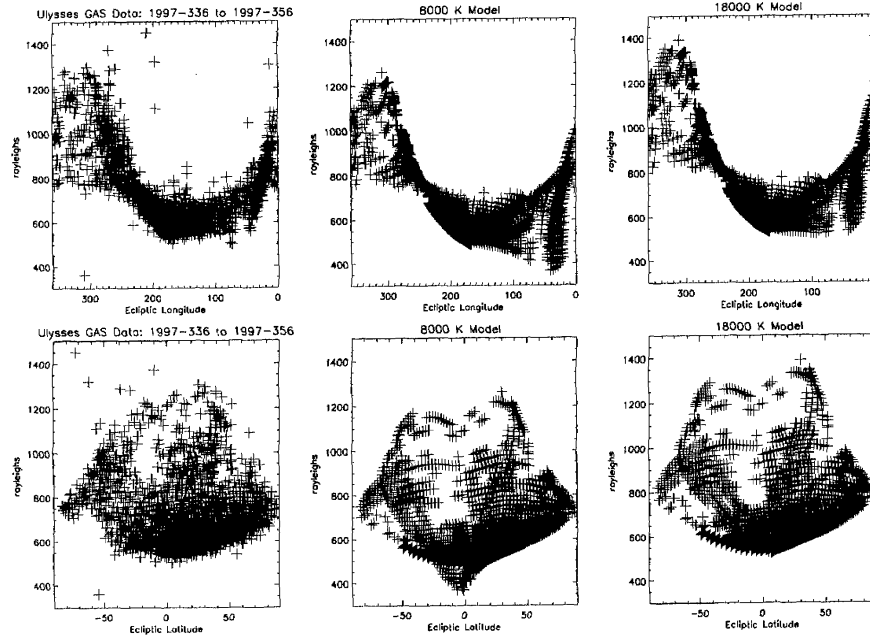


Figure 5. Left: *Ulysses* GAS  $L\alpha$  data from 1997. Middle: an 8000 K model using the fit for H lifetime (Figure 4) has too much downwind groove. Right: 18 000 K improves the downwind fit near the ecliptic.

This GAS map was obtained from ecliptic latitude  $7^\circ$ , ecliptic longitude  $156^\circ$ , and a heliocentric distance of 5.36 AU.

The H charge exchange rate  $R$  depends on solar wind proton density  $n_p$ , velocity  $v$ , and the velocity-dependent cross-section  $\sigma$ :  $R = n_p v \sigma(v)$ . *High speed solar wind has a lower charge exchange cross-section (Barnett et al., 1990) than low-speed wind.* The model rate  $R(s^{-1})$  at 1 AU as a function of heliographic latitude  $\theta$  in radians is:

$$R(\theta) = 2.45 \times 10^{-7} + 3.95 \times 10^{-7} e^{-6.37 \sin^2 \theta} s^{-1} \quad (2)$$

based on SWOOPS data from when *Ulysses* was 2–5.4 AU from the Sun (McComas et al., 1999, Equation 3(a); Pryor et al., 1998b; Summanen et al., 1997):

H lifetimes are shown in Figure 4, along with the application of Equation (2) to GAS upwind data. Figure 5 tests models at different  $T$  with the full GAS map.

#### 4. *Ulysses* GAS Conclusions for the Last Solar Minimum

–GAS upwind data from December 1997 show a plateau and weak groove near the ecliptic. The plateau/groove shape can be modeled with SWOOPS solar wind data.

–Data/Model residuals imply greater solar wind mass flux in south than north, as noted in SWOOPS data (McComas *et al.*, 2000a).

–Hot models need  $T > 8000$  K to remove the downwind groove.  $T = 18\,000$  K is ok.

–GAS finds  $T(\text{H}) \sim 18\,000$  K; GAS previously found  $T(\text{He}) \sim 6100\text{--}7000$  K (Witte *et al.*, 1996). The difference implies H heating in the outer heliosphere.

##### 4.1. FUTURE PLANS

We will study solar cycle changes in charge-exchange rates, using new SWOOPS data to see if  $A \sim 0$  is plausible at solar maximum.

#### References

- Ajello, J. M. *et al.*: 1994, *Astron. Astrophys.* **289**, 283–303.  
 Barnett, C. F.: 1990, Tech. Rep. ORNL-6086, Vol. 1, Oak Ridge National Laboratory, Oak Ridge, TN.  
 Bertaux, J. L. *et al.*: 1985, *Astron. Astrophys.* **150**, 1.  
 Bertaux, J. L. *et al.*: 1997, *Sol. Phys.* **175**, 737.  
 Costa, J. *et al.*: 1999, *Astron. Astrophys.* **349**, 660.  
 Hord, C. W. *et al.*: 1992, *Space Sci. Rev.* **60**, 503.  
 McComas, D. J. *et al.*: 1999, *Geophys. Res. Lett.* **26**, 2701.  
 McComas, D. J. *et al.*: 2000a, *J. Geophys. Res.* **105**, 10 419.  
 McComas, D. J., Gosling, J. T., and Skoug, R.: 2000b, *Geophys. Res. Lett.* **27**, 2437.  
 McComas, D. J., Gosling, J. T., and Skoug, R. M.: 2000c, at the 34th ESLAB Symposium.  
 Pryor, W. R. *et al.*: 1992, *Astrophys. J.* **394**, 363.  
 Pryor, W. R. *et al.*: 1996, *Geophys. Res. Lett.* **23**, 1893.  
 Pryor, W. R. *et al.*: 1998a, *J. Geophys. Res.* **103**, 26 833.  
 Pryor, W. R., Witte, M., and Ajello, J. M.: 1998b, *J. Geophys. Res.* **103**, 26 813.  
 Summanen, T., Lallement, R., and Quemerais, E.: 1997, *J. Geophys. Res.* **102**, 7051.  
 Thomas, G. E.: 1978, *Ann. Rev. Earth Planetary Sci.* **6**, 173.  
 Witte, M. *et al.*: 1992, *Astron. Astrophys. Suppl. Ser.* **92**, 333.  
 Witte, M., Banaszkiewicz, M., and Rosenbauer, H.: 1996, *Space Sci. Rev.* **78**, 289.